Cell Stem Cell
Article

Global Transcription in Pluripotent Embryonic Stem Cells

Sol Efroni,[1,8] Radharani Duttagupta,[2] Jill Cheng,[2,10] Hesam Dehghani,[3,11] Daniel J. Hoeppner,[4] Chandravanu Dash,[5] David P. Bazett-Jones,[3] Stuart Le Grice,[5] Ronald D.G. McKay,[4] Kenneth H. Buetow,[1] Thomas R. Gingeras,[2] Tom Misteli,[7,9,*] and Eran Meshorer[6,8,9,*]

[1]National Cancer Institute Center for Bioinformatics, National Institutes of Health, Rockville, MD 20852, USA
[2]Affymetrix, Inc., 3380 Central Expressway, Santa Clara, CA 95051, USA
[3]The Hospital for Sick Children, Toronto, ON M5G 1X8, Canada
[4]National Institute of Neurological Disorders and Stroke, National Institutes of Health, Bethesda, MD 20852, USA
[5]National Cancer Institute, National Institutes of Health, Frederick, MD 21702, USA
[6]Department of Genetics, Institute of Life Sciences, The Hebrew University of Jerusalem, Jerusalem 91904, Israel
[7]National Cancer Institute, National Institutes of Health, Bethesda, MD 20892, USA
[8]These authors contributed equally to this work.
[9]These authors contributed equally to this work as senior authors.
[10]Present address: Novartis Institutes for BioMedical Research, 4560 Horton Street, Emeryville, CA 94608, USA.
[11]Present address: Institute of Biotechnology, Ferdowsi University of Mashhad, Mashhad 91775-1793, Iran.
*Correspondence: meshorer@cc.huji.ac.il (E.M.), mistelit@mail.nih.gov (T.M.)
DOI 10.1016/j.stem.2008.03.021

SUMMARY

The molecular mechanisms underlying pluripotency and lineage specification from embryonic stem cells (ESCs) are largely unclear. Differentiation pathways may be determined by the targeted activation of lineage-specific genes or by selective silencing of genome regions. Here we show that the ESC genome is transcriptionally globally hyperactive and undergoes large-scale silencing as cells differentiate. Normally silent repeat regions are active in ESCs, and tissue-specific genes are sporadically expressed at low levels. Whole-genome tiling arrays demonstrate widespread transcription in coding and noncoding regions in ESCs, whereas the transcriptional landscape becomes more discrete as differentiation proceeds. The transcriptional hyperactivity in ESCs is accompanied by disproportionate expression of chromatin-remodeling genes and the general transcription machinery. We propose that global transcription is a hallmark of pluripotent ESCs, contributing to their plasticity, and that lineage specification is driven by reduction of the transcribed portion of the genome.

INTRODUCTION

Embryonic stem cells (ESCs) are unique in their capacities to self-renew and to initiate differentiation into any cell type of the three germ layers. These opposing abilities are in part brought about by the presence of stem cell-specific factors (Hochedlinger et al., 2005; Hough et al., 2006; Nichols et al., 1998; Pan et al., 2002; Scholer et al., 1990; Takahashi and Yamanaka, 2006). During differentiation, lineage-specific transcription factors activate the expression of specific sets of genes that are required for each specific lineage to form hierarchical transcription networks (Szutorisz and Dillon, 2005).

In addition to control by specific transcription factors, epigenetic regulation has recently emerged as a key mechanism in pluripotency and lineage specification (Azuara et al., 2006; Bernstein et al., 2006; Boyer et al., 2006b; Buszczak and Spradling, 2006; Gan et al., 2007; Meshorer, 2007; Meshorer and Misteli, 2006). ESC chromatin is characterized by several specific features, which distinguish it from that of somatic and differentiated cells (Niwa, 2007). ESC chromatin is morphologically distinct in that heterochromatin is organized in larger and fewer domains, which become smaller, more abundant, and hypercondensed as cells differentiate (Aoto et al., 2006; Kobayakawa et al., 2007; Meshorer and Misteli, 2006; Park et al., 2004). Another characteristic feature of stem cell chromatin is the altered binding of chromatin proteins (Meshorer et al., 2006). Architectural chromatin proteins such as the heterochromatin component HP1, the linker histone H1, and core histones display hyperdynamic and looser binding to chromatin in undifferentiated ESCs compared to differentiated cells. Hyperdynamic binding is exclusively found in pluripotent cell types, but not in lineage-committed but undifferentiated cells, indicating that dynamic chromatin is associated with pluripotency rather than differentiation per se (Meshorer et al., 2006). ESCs also contain unique histone modification patterns (Spivakov and Fisher, 2007). Extensive regions of the genome are bivalently marked by transcriptionally repressive H3K27me3, but at the same time contain the transcription-associated histone modification H3K4me3 (Azuara et al., 2006; Bernstein et al., 2006). It has been proposed that these "bivalent" domains silence developmentally regulated genes in ESCs while keeping them poised for activation as cells enter the various differentiation pathways (Bernstein et al., 2006; Jorgensen et al., 2006). Repression of H3K27me3 appears to be mediated by the polycomb repression complex 2 (PRC2), which is associated with a significant number of developmental regulators (Boyer et al., 2006b; Lee et al., 2006).

A striking commonality among the ESC-specific chromatin properties is that they are all indicative of transcriptionally active chromatin. We have suggested that ESC genomes are globally

transcriptionally hyperactive and express large regions of the genome, possibly indiscriminately and at low levels (Meshorer and Misteli, 2006). Here we have directly tested this hypothesis and demonstrate global, low-level transcriptional activity in the ESC genome. We find elevated levels of total RNA and mRNA in pluripotent mouse ESCs, and we show that undifferentiated ESCs express repetitive sequences, mobile elements, as well as lineage- and tissue-specific genes at low levels. Using whole-genome mouse tiling arrays, we show that a larger fraction of the genome is active in ESCs compared to differentiating cells. The global transcriptional activity of the ESC genome is accompanied by elevated levels of chromatin-remodeling proteins and the global transcription machinery, but not histone-modifying activities. Modulation of several specific chromatin-remodeling activities in ESCs interferes with their proliferation and differentiation. Our results identify global, low-level genome activity as a hallmark of ESC genomes, and they suggest that loss of pluripotency and lineage specification involves reduction of the actively transcribed portion of the genome.

RESULTS

Hallmarks of Transcriptionally Active Chromatin in ESCs

ESC chromatin is characterized by several distinct properties. For one, in ESCs, heterochromatin is organized in larger and fewer domains, which become smaller, more abundant, and hypercondensed as cells differentiate (Aoto et al., 2006; Kobayakawa et al., 2007; Meshorer and Misteli, 2006; Park et al., 2004). To characterize the ultrastructure of ESC chromatin, we compared by quantitative electron microscopy undifferentiated mouse R1 ESCs with neuronal progenitor cells (NPCs) derived from them by in vitro differentiation (see Figures S1A and S1B available online). Consistent with global decondensation in ESCs, the majority of chromatin appears homogeneous and decondensed in undifferentiated pluripotent cells (Figure S1A, left). In contrast, in R1 NPCs chromatin is heterogeneous in appearance and distinct heterochromatin domains are frequently present (Figure S1A, middle; Meshorer et al., 2006).

In addition to morphological differences, chromatin in ESCs is molecularly distinguished by a set of bivalent histone modifications of both an active and a repressive state (Azuara et al., 2006; Bernstein et al., 2006). To extend these studies, we compared the status of a series of histone modifications in undifferentiated R1 ESCs and NPCs derived from them (Figures S1C and S1D). We find enrichment of several histone marks commonly associated with active chromatin, including H3K4me3, H3K9ac, H3K14ac, H3K36me2, and H3K36me3 in ESCs compared to ESC-derived NPCs (Figures S1C and S1D). The significantly elevated levels of the RNA Pol II-mediated elongation-associated histone modification H3K36me2 (Bannister et al., 2005) (Figure S1C) are further suggestive of increased transcriptional activity in ESCs. The opposite behavior was observed for histone marks associated with transcriptional silencing. H4K20me2 is unchanged, but the heterochromatin-associated modification H3K9me3 is dramatically underrepresented in ESCs (Meshorer et al., 2006), consistent with the absence of heterochromatin domains in ESCs (Figures S1A and S1B; Meshorer et al., 2006). Similarly, a further hallmark of transcriptionally repressed genome regions, DNA methylation of cytidine (5meC) is also significantly reduced in ESCs compared to NPCs (Bibikova et al., 2006) (Figures S1C and S2).

Elevated Global Transcription in ESCs

The characteristic properties of ESC chromatin, including global decondensation, looser binding of architectural chromatin proteins, and enrichment of active histone modifications, are all hallmarks of transcriptionally active chromatin. Based on these observations, we hypothesized that ESCs are globally transcriptionally more active than differentiated cells (Meshorer and Misteli, 2006). To directly test this hypothesis, we measured global transcriptional activity by [^{3}H]uridine incorporation (Kimura et al., 2002) in undifferentiated ESCs and 7 day NPCs derived from ESCs by in vitro differentiation (Lee et al., 2000; Meshorer et al., 2006). Strikingly, total RNA and mRNA levels (5%–10% of total RNA) normalized to DNA content were almost 2-fold higher in ESCs compared to NPCs (Figure 1A, $p < 0.005$ and 0.05, respectively, Mann-Whitney two-tailed test). Higher levels of incorporated [^{3}H]uridine were not due to increased RNA stability in ESCs because RNA decay rates were comparable in ESCs and NPCs as demonstrated by pulse-chase labeling of newly synthesized total RNA (Figure 1B) and mRNA (Figure 1C).

The elevated transcriptional activity in undifferentiated ESCs could either be due to the activity of a specific set of genes or might alternatively reflect global activation of the genome in ESCs. To begin to distinguish between these possibilities, we analyzed the activity status of satellite repeat sequences, LINEs, SINEs, and several retrotransposons (Martens et al., 2005), which are normally repressed in differentiated cells. Transcription of all elements, including major and minor satellite repeats, LINEs, and SINEs, was significantly higher in ESCs than in ESC-derived NPCs (Figure 1D; $p < 0.05$; normalized to the constantly expressed *Cyclophilin-B* mRNA). While these elements were detected at low levels in NPCs, their expression was increased by 2- to 10-fold in ESCs (Figure 1D). We obtained similar results when undifferentiated ESCs were compared to other cell types, such as MEFs or differentiated C2C12 muscle cells (data not shown). To exclude the trivial possibility that the detection of these transcripts by RT-PCR was due to their expression in only a small subpopulation of cells in the ESC population, we visualized major satellite repeat expression in undifferentiated (Figure 1E, ESC) and differentiated (Figure 1E, NPC) ESCs by RNA fluorescence in situ hybridization. Expression of major satellite repeats was detected in 83 ± 23% of the undifferentiated ESCs but only in 23 ± 11% of NPCs (Figure 1E). When ESCs were pretreated with RNase, the signal was abolished (Figure 1E, +RNase), whereas DNase treatment left the signal intact (Figure 1E, +DNase). These results show that undifferentiated ESCs express regions of the genome that are normally silenced in differentiated cells.

Low-Level Expression of Tissue-Specific Genes in ESCs

To ask whether transcription of silent genome regions was limited to repeat sequences or was a general property of the ESC genome, we probed the transcription status of specific genes using RT-PCR. We selected several tissue-specific genes and genes associated with terminal differentiation, which are not expected to be expressed in undifferentiated ESCs (Table S1). In order to avoid false positives originating from DNA contamination, all

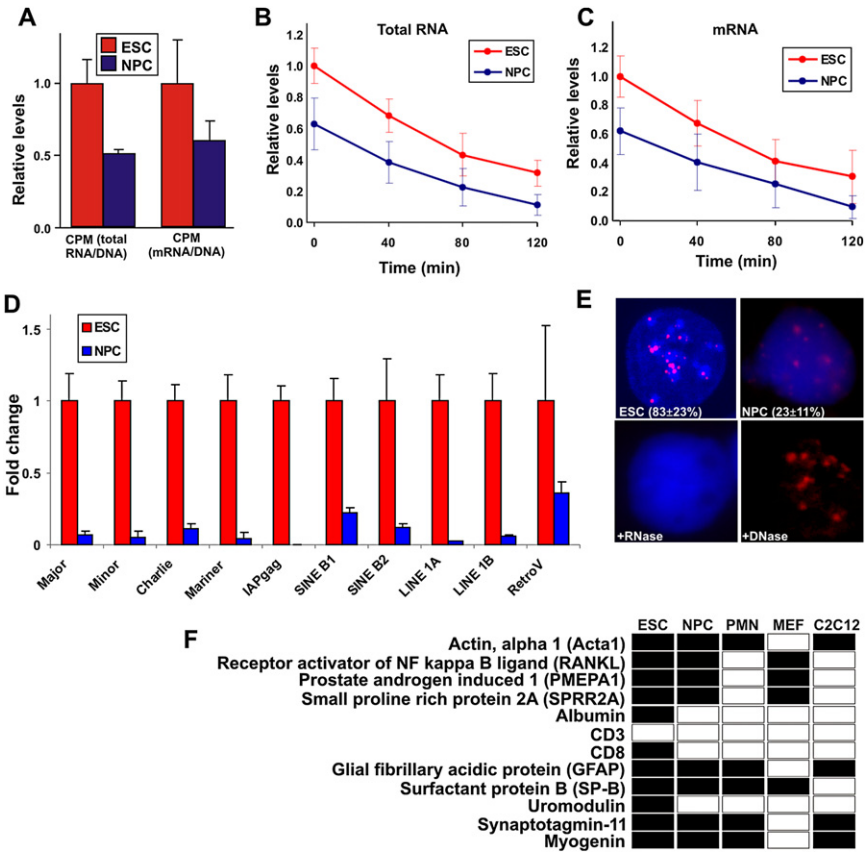

Figure 1. Elevated Global Transcription in ESCs

(A) Total RNA transcriptional activity (left) and mRNA transcriptional activity (right) in ESCs (red) and NPCs (blue). Cells were incubated with ^{3}H-labeled uridine for 4 hr. Values represent averages ± SD from three experiments.

(B and C) As in (A), but following 2 hr of incubation, [^{3}H]uridine was removed and fresh medium supplemented with 0.125 μM actinomycin-D was added for an additional 2 hr. Samples were collected every 40 min, and transcriptional activity of both total RNA (B) and mRNA (C) levels was determined.

(D) Real-time quantitative PCR of the indicated repeat sequences and transposable and retroviral elements in ESCs (red) and NPCs (blue) normalized against *Cyclophilin B*. Values represent averages ± SD from three independent experiments.

(E) RNA-FISH for the major satellite repeat using Cy3-labeled locked nucleic acid (LNA) probes in embryonic stem cells (ESC) and ESC-derived neuronal progenitor cells (NPC). When ESCs were pretreated with RNase A, signal was abolished (+RNase), while DNase I treatment retained the signal (DNase). Values represent averages ± SD from three experiments. At least 50 cells were scored per experiment.

(F) Lineage-specific transcription in undifferentiated ESCs. Shown is a detection table (black, detected; white, undetected) of a selection of lineage-specific genes detected by RT-PCR in undifferentiated ESCs, NPCs, ESC-derived postmitotic neurons (PMN), MEFs, or differentiated C2C12 cells. Genes were considered not expressed when undetected in two independent experiments. Several genes required reamplification for detection (Figure S3). All samples were treated similarly. For copy number determination, see the Supplemental Experimental Procedures.

PCR primers were designed to flank long introns, so that the genomic products would be significantly longer than the cDNA products (Table S1). Transcripts for 11 out of 12 lineage-restricted genes were detected in undifferentiated ESCs (Figure 1F). The transcription level of these genes was very low, with an estimated 0.25–20 copies per cell as determined by direct comparison with known quantities of plasmid cDNA (Supplemental Experimental Procedures), suggesting their transcription likely occurs stochastically within the population. The low abundance prevented accurate quantification by real-time PCR in most cases, and some required reamplification (Figure S3A). However, in the cases for which we were able to quantitatively compare transcription levels in ESCs, 7 day NPCs, and ESC-derived fully differentiated postmitotic neurons (PMNs) by quantitative real-time PCR, transcription levels decreased during differentiation (Figure S3B). In 7 day NPCs, 8 of 12 genes were still detected, but this number dropped to 5 in PMNs (Figure 1F). As a control, we tested several differentiated cell lines. Most of the genes analyzed were silenced in MEFs and C2C12 muscle cells, except the ones specific to that particular lineage, such as *Acta1* and *Myogenin* in C2C12 cells and *SPRR2A* in MEFs. Interestingly, comparison with publicly available chromatin immunoprecipitation followed by genomic sequencing (ChIP-seq) data (Mikkelsen et al., 2007) revealed that all detected genes (except *SPRR2A*, for which ChIP data were not available) were marked with higher levels of both H3K4me3 and H3K27me3 in undifferentiated ESCs than in NPCs, and the H3K27me3:H3K4me3 ratio increased following differentiation (Figures S4A and S4B), supporting increased silencing of lineage-specific genes in the differentiated state. Attempts to detect protein products from these transcripts using western blotting yielded negative results (data not shown).

Genome-wide Transcriptional Activity in ESCs

To systematically assess the transcriptional status of the entire genome and to extend our analysis to noncoding genome regions, we used an Affymetrix whole-genome mouse tiling array at 30 bp resolution to compare genome-wide transcription profiles in pluripotent ESCs and in ESC-derived NPCs (see the Experimental Procedures for details). Microarray analysis was validated by the detection of downregulation of several stem cell-specific genes, including *Oct4* and *Sox15*, during differentiation, whereas expression of neuronal genes, including *Sox4* and *Sox11* (Bergsland et al., 2006), was increased as confirmed by qPCR (Figures S5A and S5B). The tissue-specific transcripts detected in ESCs by RT-PCR showed low-level or no transcription on the tiling array, indicating the sensitivity limits of the microarray (Figure S5C). A detailed list of gene and transcript

lengths, untranslated region (UTR) length, and their average lengths are given in Table S2. To ask whether the genome of undifferentiated ESCs is globally transcriptionally more active, we first compared the number of positive probes on microarrays hybridized with poly(A)$^+$ RNA from ESCs or from ESC-derived 7 day NPCs. We used the number of single positive probes as a general surrogate for transcriptional activity. In support of increased global transcriptional activity in ESCs, the number of positive probes was significantly elevated in ESCs compared to NPCs. While in ESCs, 1,041,879 probes displayed intensity values above threshold (defined as 90% noise level, calculated using the mismatch probes data; see the Experimental Procedures for details); this number was reduced to 838,787 positive probes in NPCs, corresponding to an ~20% decrease ($p < 10^{-5}$, two-tailed Student's t test). The number of reduced probes is an underestimate because equal amounts of RNA rather than RNA from equal number of cells were hybridized and only RNAs of more than 200 nt transcripts in length were purified for use in hybridization. In addition, a stringent threshold was used to avoid measurements of false-positive probes.

The reduction of detected probes occurred across all regions of the genome, including intergenic (Figure 2A), intronic (Figure 2B), and exonic (Figure 2C) domains. Importantly, the reduction was evident as early as 24 hr after the withdrawal of LIF, demonstrating that the reduction in transcriptional activity is not restricted to a particular lineage and was not due to more rapid proliferation of undifferentiated ESCs, because ESCs after 24 hr withdrawal of LIF are still highly proliferative. The degree of reduction varied among chromosomes but was typically between 20% and 50% in NPCs (Figure 2). Global transcriptional reduction was most prominent in intergenic and intronic regions. In these regions, probe counts were significantly reduced in 9–15 of the 21 chromosomes by 24 hr and in 12–17 of the 21 chromosomes by 7 days. The remaining chromosomes did not show significant changes (Figures 2A and 2B). In exonic regions, 5 chromosomes displayed reductions at the 24 hr time point and 11 chromosomes showed reduced counts in NPCs (Figure 2C). Interestingly, in NPCs 2 chromosomes (1 and 12) showed significantly elevated counts in exonic regions only. These are likely due to a disproportionately high number of differentiation-induced genes on these chromosomes, including *Sox11*, *Sox17*, and many others (Table S3). The overall reduction of active probes was not due to elevated levels of ribosomal genes, as the rDNA-bearing chromosomal regions are not represented on the array. To verify that the elevated number of probes in ESCs was not due to increased background noise, we analyzed the distribution of the probes that were exclusively present in ESCs but not in NPCs. Slightly more than 50% of probes were clustered in groups of three or longer, corresponding to 100 bp or longer transcripts (Figure S6). Comparison of the size distribution of the positive probes with a random distribution using computer-assisted statistical simulations suggested that they were contiguous transcripts ($p < 10^{-6}$).

The more global transcriptional activity in ESCs was also evident from inspection of selected intergenic and intronic regions (Figure 3). Some intergenic regions in ESCs exhibited "transcription bursts" displaying intermittent active and silent regions, which were reduced to near threshold levels in NPCs (Figure 3A). In other cases, intergenic regions were active over

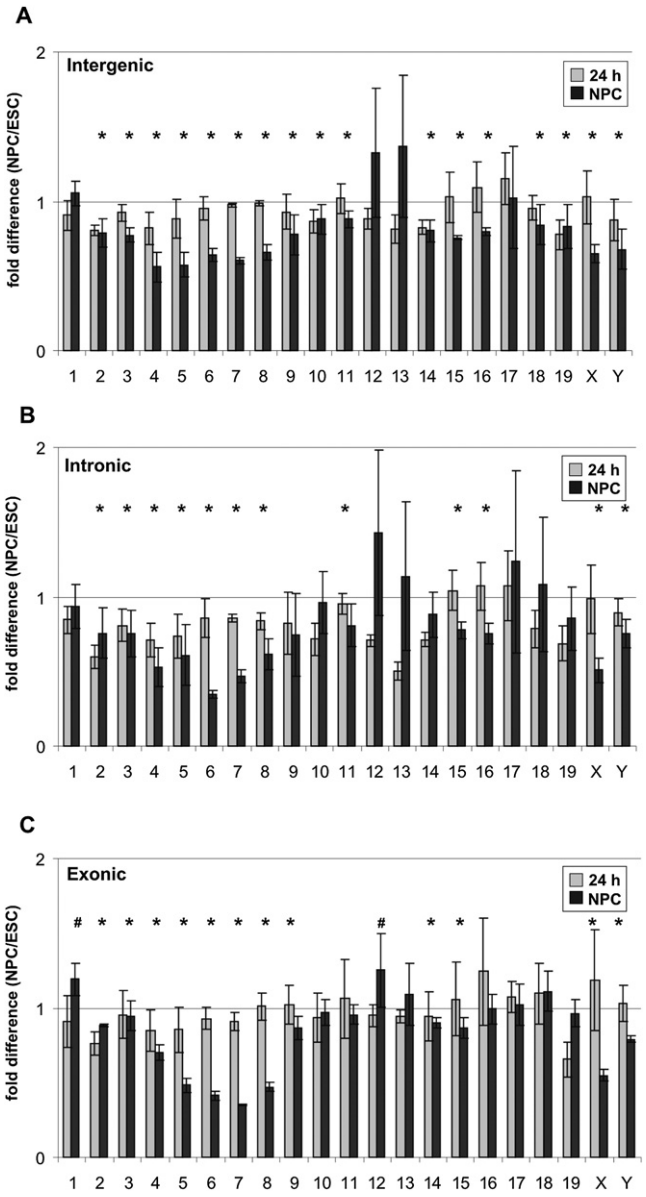

Figure 2. Whole-Genome Mouse Tiling Array Analysis

(A–C) Comparison of average fold difference (±SD) for positive probes from each chromosome between undifferentiated ESCs, cells 24 hr after LIF withdrawal (gray columns), and NPCs (black columns). The fold difference is depicted relative to the 1.0-fold change shown as a straight line for intergenic regions (A), intronic regions (B), and exonic regions (C). Data are from three independent experiments. Asterisks denote significant reduction, and number sign (#) denotes significant increase between ESCs and NPCs ($p < 0.017$). P values were estimated by one-side hypothesis testing, adjusted with Bonferroni correction for multiple comparisons.

large contiguous stretches in ESCs and activity was dramatically reduced over the entire region in NPCs (Figure 3B). Some regions were characterized by "transcriptional islands" in which parts of a region were active in both ESCs and NPCs (Figure 3C). Significant transcription occurred in many cases along entire introns in ESCs (Figure 3D) or was often confined to a limited region of varying extent within the intron in ESCs,

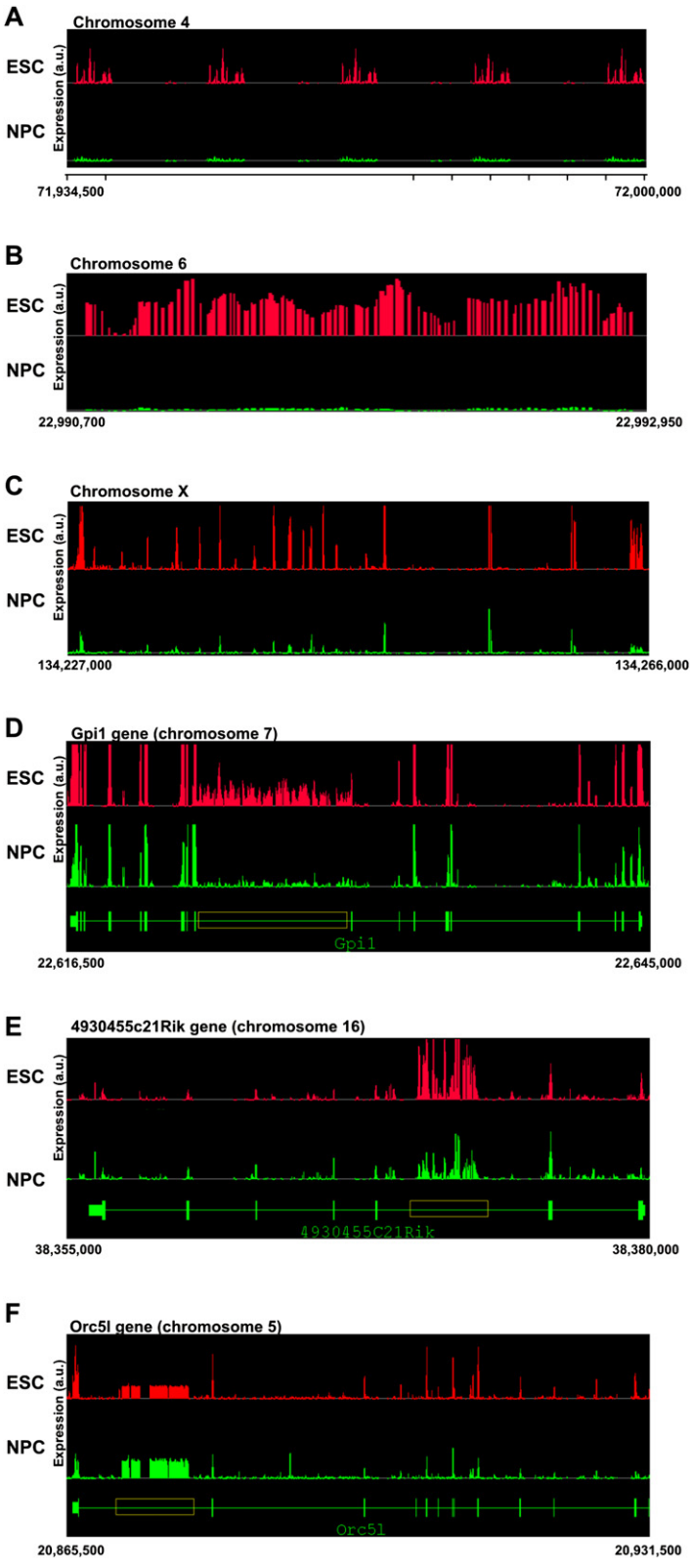

Figure 3. Elevated Intergenic and Intronic Transcription Patterns in ESCs

Composite graphs depicting signal intensity from the independent biological replicas represent probe intensity per genomic coordinates. All represented coordinates are in the mm.NCBIv33 version of the mouse genome and are indicated below each panel. Y axis denotes arbitrary units of expression.

(A–C) Intergenic transcription. (A) An ~65 kb intergenic region on chromosome 4 displaying repetitive bursts of transcription in ESCs (red, top), but not in NPCs (green, bottom). (B) A 2250 bp intergenic region on chromosome 6, which is active in ESCs (red, top) but not in NPCs (green, bottom). (C) A 29 kb intergenic region on chromosome X, where parts are active in both ESCs and NPCs and parts are active in ESCs only.

(D–F) Intronic transcription. (D) The annotated region of the *Gpi1* gene (~28 kb) on chromosome 7 (green, bottom) shows intronic transcription (yellow box, >7.5 kb) in both ESCs (red, top) and NPCs (green, middle), but transcription level is considerably higher in ESCs. (E) The annotated region of the *4930455C21Rik* gene (~25 kb) on chromosome 16 (green, bottom) shows a burst of transcription inside the fifth intron in both ESCs (red, top) and NPCs (green, middle). Despite higher expression of the *4930455C21Rik* gene in NPCs, intronic transcription is higher in ESCs. Note that unlike *Gpi1*, exons in this case are active at lower levels than the intronic transcription. (F) The annotated region of the *Orc5l* gene (~66 kb) on chromosome 5 (green, bottom). A long intronic region (yellow box, >8 kb) inside the *Orc5l* gene is active. The *Orc5l* gene itself is also active, and the intronic transcription is lower than the exonic transcription. In this example, intronic transcription is higher in NPCs (green, middle) than in undifferentiated ESCs (red, top).

but was significantly reduced in NPCs (Figures 3E and 3F). These reductions were specific, as numerous intronic regions were more highly expressed in NPCs (Figure 3F). These analyses of intronic and intergenic regions point to a widespread elevated genomic transcriptional activity in undifferentiated ESCs.

Elevated Transcription Levels in Active Genome Regions of ESCs

Inspection of regions that were active both in ESCs and in NPCs often indicated higher transcription levels in ESCs (Figure 3E), suggesting that the increased overall transcription level might not only be due to additional active regions, but also generally higher levels of transcription in constitutively active regions. To test this possibility, we analyzed the expression level of all probes that were active in both undifferentiated ESCs and cells differentiated for either 24 hr or 7 days (NPCs). By 24 hr, between 14 and 19 chromosomes displayed a higher number of downregulated than upregulated probes in all regions (Figures 4A–4C, left). After 7 days, both intergenic and intronic regions displayed a higher number of downregulated than upregulated probes on all chromosomes (Figures 4A and 4B, right). Exonic regions displayed the same general trend of a higher number of downregulated probes in 19 of the 21 chromosomes (Figure 4C, right). The two remaining chromosomes (1 and 12) showed a higher number of upregulated probes, in agreement with the number of active probes in these chromosomes (see Figure 2C) and the higher number of differentiation-induced genes. The same trend was observed when the 24 hr time point was compared with NPCs (Figure S7). These data indicate that the activity of genomic regions that are active in both

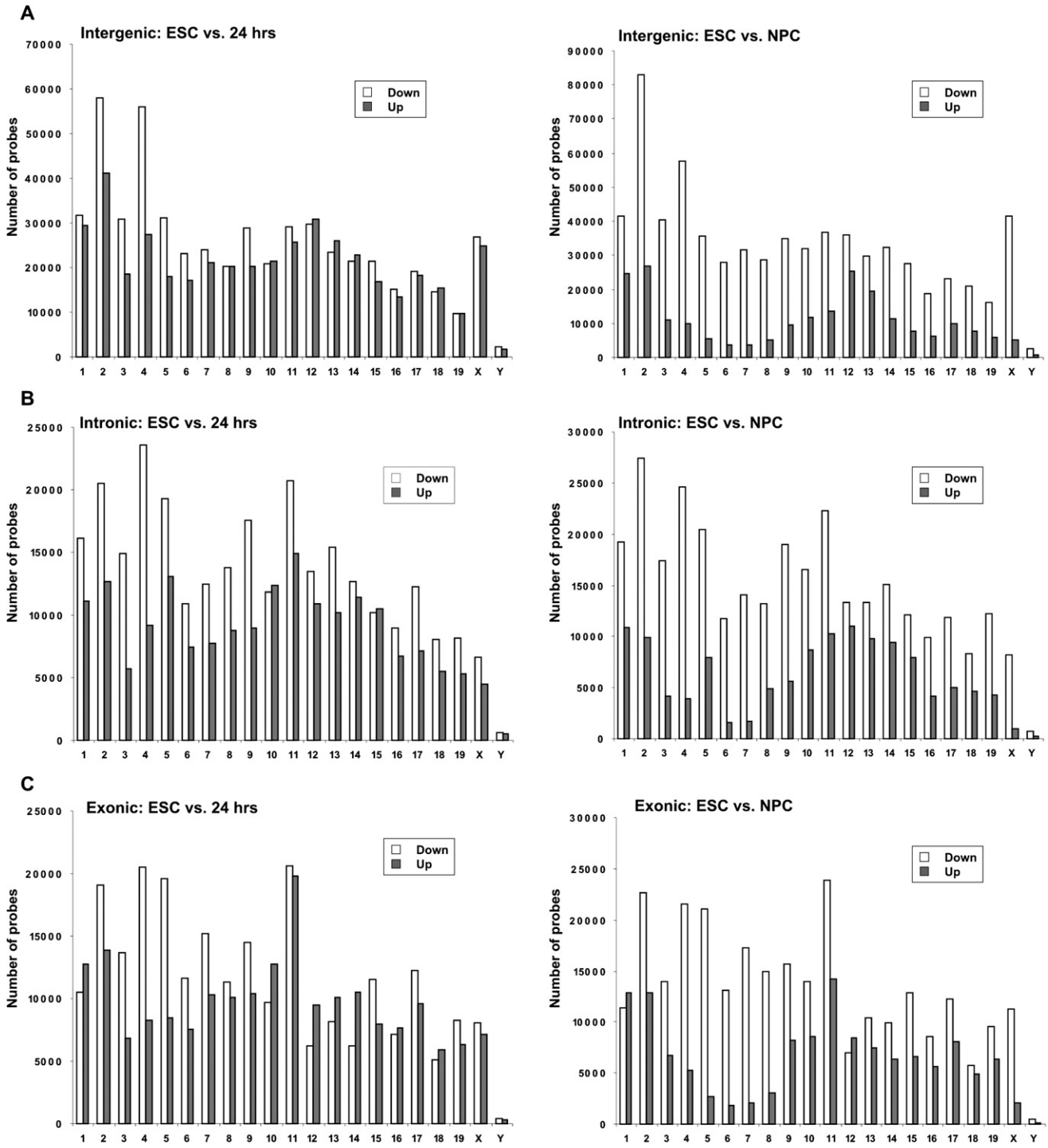

Figure 4. Global Expression Changes during ESC Differentiation

(A–C) Comparison of positive probes between ESCs and cells 24 hr after LIF withdrawal (left) or between ESCs and neuronal progenitor cells (NPC, right). Total number of downregulated and upregulated probes is depicted as white and gray bars, respectively, for intergenic regions (A), intronic regions (B), and exonic regions (C) for all mouse chromosomes. Only probes that were positive in both time points were used for this analysis. Data represent the average of three independent experiments.

undifferentiated and differentiating ESCs is higher in the undifferentiated state. In sum, based on the genome-wide analysis of active probe number, probe distribution, and signal level, we conclude that the genome of undifferentiated ESCs exhibits global transcriptional activity, which becomes restricted during differentiation.

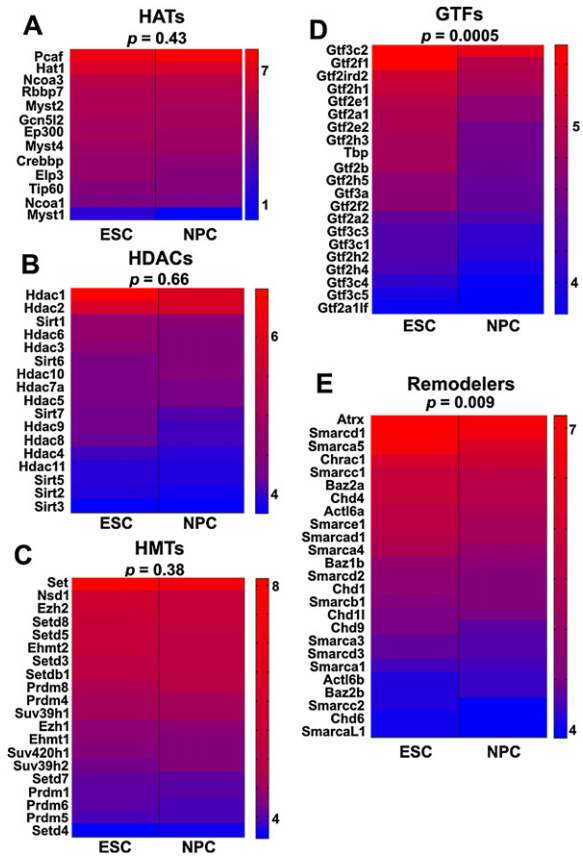

Figure 5. Disproportionate Overrepresentation of General Transcription Factors and Chromatin-Remodeling Genes in Undifferentiated ESCs

(A–E) Transcription level heat maps of different groups of genes that are associated with transcription and regulation of chromatin, including histone acetyltransferases (A), histone deacetylases (B), histone methyltransferases (C), GTFs (D), and chromatin-remodeling proteins (E). Gene names are given on the left of each map; P values (binomial hypothesis testing) are indicated on top. Chromatin-remodeling factors and GTFs are disproportionately expressed in ESCs. Heat maps were generated using microarray signal levels displayed as arbitrary units. Red-to-blue corresponds to high-to-low signal intensity.

Elevated Transcription of Chromatin-Remodeling Factors and General Transcription Factors in Undifferentiated ESCs

We hypothesized that the global changes in chromatin structure and the low-level transcription of large regions of the genome may be brought about by differences in the levels of chromatin proteins. To determine the basis of global transcription in ESCs, we performed a genome-wide comparison of the transcript levels of known general transcription factors (GTFs), chromatin-remodeling factors, and several types of histone-modifying activities including histone acetyltransferases (HATs), histone deacetylases (HDACs), and histone methyltransferases (HMTs) in ESCs and NPCs (Figure 5 and Figure S8). To compare changes in the transcription levels of these groups of genes to the entire transcriptome, we first examined the complete set of annotated genes on the tiling arrays. Based on lower intensities of constitutive probes, 54% of all genes were reduced during differentiation into NPCs, 38% were elevated, and 8% of the genes were unchanged or undetected at both time points. We then compared these numbers to the expression patterns of the various groups of chromatin proteins. While all histone modifiers, including HATs (Figure 5A), HDACs (Figure 5B), and HMTs (Figure 5C), showed a similar reduction in their transcription levels as the complete transcriptome (p = 0.34, 0.66, and 0.59, respectively), GTFs (Figure 5D) and chromatin-remodeling genes (Figure 5E) displayed a statistically significant more pronounced reduction in their transcription level (p = 0.0005 and 0.009 compared to all other genes, respectively), suggesting a disproportionately high level of expression of GTFs and chromatin-remodeling proteins in ESCs. Out of 25 detectable chromatin-remodeling genes, 20 were significantly downregulated in NPCs and 5 were slightly elevated. Among the 21 detectable GTFs, 19 were downregulated in NPCs and only 2 were slightly elevated (Figure 5E). The expression patterns for the chromatin-remodeling factors were confirmed by qRT-PCR (Table S4 and Figure S9). Consistent with the transcriptional downregulation of GTFs and chromatin remodelers, their protein levels were reduced in NPCs compared with ESCs (Figure S10).

Reduction of Chromatin-Remodeling Activity Impairs ESC Proliferation and Differentiation

To test whether the overrepresentation of chromatin-remodeling factors was functionally relevant for ESCs and their differentiation, we selectively tested the effect of knockdown of the SWI/SNF remodeling component *Brg1* (*Smarca4*), the SWI/SNF component *Smarcd2*, and the ISWI-related chromodomain helicase DNA binding protein 1-like (*Chd1l*) by RNAi. Knockdown for Brg1 factor was confirmed by western blotting (Figure 6A), and for *Smarcd2* and *Chd1l* knockdown was confirmed by quantitative real-time PCR due to the absence of antibodies (Figure 6B). RNAi against luciferase was used as a negative control (Figure 6). ESCs treated with *Brg1* siRNAs displayed marked reduction in both their proliferation and differentiation capacities (Figures 6A, 6C, and 6D). After 96 hr of *Brg1* siRNA treatment, the proliferation rate was roughly 60% of that of luciferase RNAi-treated cells (Figure 6C, top left). In addition, while luciferase siRNA-treated cells generated nestin-positive NPCs at a rate of 74%, this number dropped to 15% in the *Brg1* siRNA-treated cells. Knockdown of *Chd1l*, which displayed the secondmost pronounced upregulation in ESCs (by 8.9 ± 3.9-fold) resulted in an ESC proliferation defect but did not appear to affect differentiation (Figures 6B and 6C), while knockdown of *Smarcd2*, which displayed the most pronounced upregulation in ESCs (by 9.6 ± 2.8-fold) resulted in no apparent phenotype (Figures 6B and 6C). Treatment with both *Smarcd2* and *Chd1l* RNAi appeared similar to *Chd1l* RNAi treatment alone (Figure 6C, bottom right). These results suggest that while some chromatin remodelers play important roles in ESC proliferation and differentiation, partial depletion of single factors may have subtle or no effects, supporting the notion that the group of chromatin-remodeling proteins, rather than individual factors, supports stem cell maintenance and pluripotency.

DISCUSSION

Our results suggest that pluripotent ESCs are characterized by elevated global transcriptional activity and that loss of

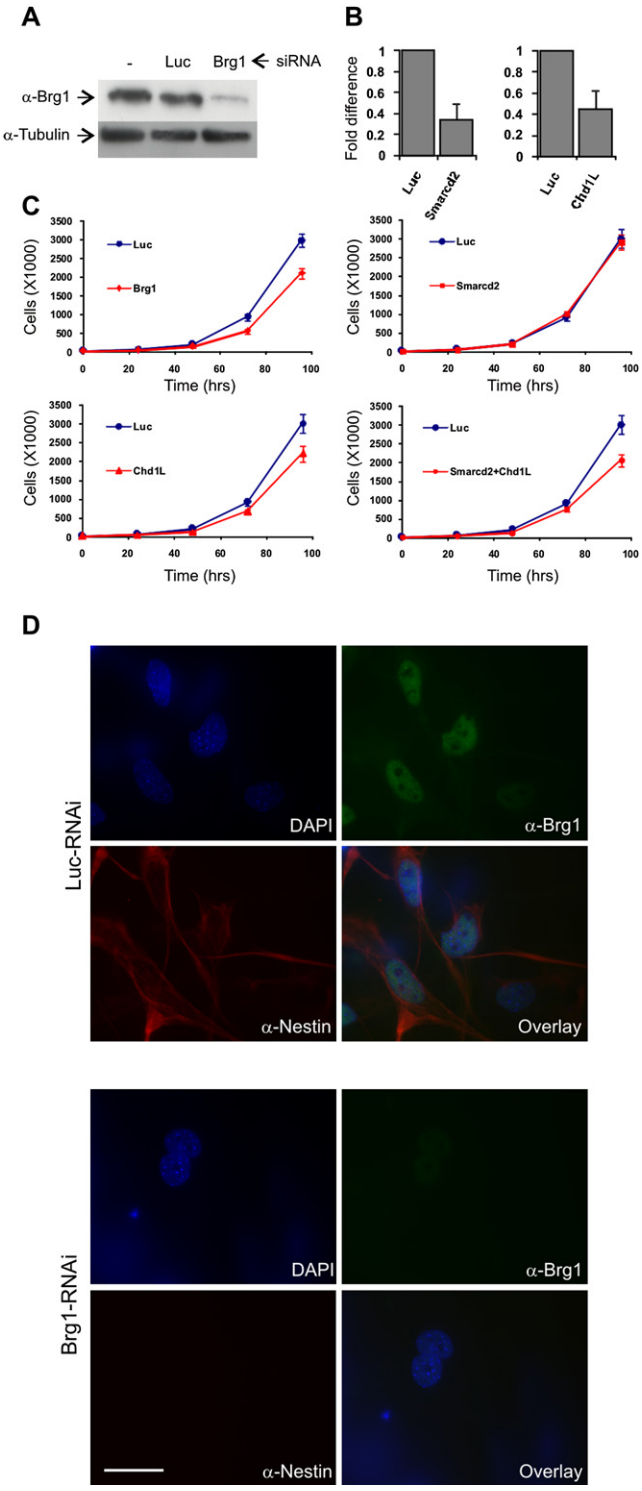

Figure 6. Knockdown of Specific Chromatin-Remodeling Factors Inhibits ESC Differentiation

(A) Knockdown of Smarca4 (Brg1) using siRNAs (SmartPool, Dharmacon). Western blot showing levels of Brg1 protein in ESCs in the absence of siRNA (left), with siRNA against luciferase (middle) and with siRNA specific to Brg1 (left). Levels of tubulin are used as control (bottom).

(B) Real-time RT-PCR of RNA levels after siRNA treatment to *Smarcd2* and *Chd1l*.

(C) Proliferation rate of luciferase siRNA-treated cells (Luc, blue lines) and of ESCs treated with siRNA against the three chromatin-remodeling factors indicated.

(D) (Top) ESC-derived NPCs treated with luciferase siRNA oligos. Brg1 is shown in green, Nestin is shown in red, and DAPI is shown in blue. Lower right panel shows overlay image. (Bottom) ESCs treated with siRNA against Brg1 fail to differentiate into NPCs. Brg1 is absent in these cells (upper right), and so is Nestin (lower left).

pluripotency and lineage specification involves reduction of the actively transcribed portion of the genome. The increased global transcriptional activity observed here is consistent with the unique properties of chromatin in ESCs, including a globally open structure, a specific set of histone modifications, and looser binding of architectural proteins (Arney and Fisher, 2004; Boyer et al., 2006a, 2006b; Buszczak and Spradling, 2006; Gan et al., 2007; Lee et al., 2006; Meshorer, 2007; Meshorer and Misteli, 2006; Meshorer et al., 2006; Szutorisz and Dillon, 2005; Szutorisz et al., 2006). Global low-level transcription in ESCs is also in line with the presence of bivalent chromatin marks of both active and repressive histone modifications on silent lineage-specific genes (Azuara et al., 2006; Bernstein et al., 2006; Mikkelsen et al., 2007). Global, possibly stochastic, transcription in ESCs is also suggested by the identification in mouse ESCs of over 40,000 different transcripts using high-coverage gene expression profiling (HiCEP) (Araki et al., 2006) as well as detection of transcription initiation at most genes in human ESCs (Guenther et al., 2007). Global genome transcriptional activity likely also occurs in human ESCs because an increased number of expressed genes have been demonstrated in human ESCs using microarray analysis (Golan-Mashiach et al., 2005). Elevated transcriptional activity and permissive expression of lineage-restricted genes have also been observed in the hematopoietic system, where expression of genes of multiple lineages was detected prior to commitment (Hu et al., 1997) and where a larger fraction of the genes is active in the undifferentiated state (Eckfeldt et al., 2005; Terskikh et al., 2003; Zipori, 2004).

The finding that GTFs and chromatin-remodeling proteins are disproportionately overexpressed in ESCs suggests that they are critical in maintaining chromatin in an open state and contribute to global transcriptional activity. Indeed, we find that loss of chromatin-remodeling factors affects ESC proliferation and differentiation in a factor-specific fashion. A critical role for chromatin-remodeling complexes in ESC differentiation has been hinted at by the observation that disruption of several of these proteins, including Brg1 (Bultman et al., 2000, 2006), Snf5 (Klochendler-Yeivin et al., 2000), SSRP1 (Cao et al., 2003), and Snf2h (Stopka and Skoultchi, 2003), results in embryonic death at the blastocyst stage before implantation, during the period when the inner cell mass (ICM), the source of all ESCs, is being formed. In *Drosophila*, chromatin remodeling is involved in germline stem cell self-renewal and differentiation (Xi and Xie, 2005). In mice, the NuRD chromatin-remodeling complex is essential for ESC differentiation (Kaji et al., 2006) and we now show here that loss of Brg1 leads to ESC differentiation defects. Furthermore, reduction of Chd1l impairs ESC proliferation. These observations are in line with the finding that the chromatin assembly factor CAF-1 is essential for heterochromatin formation in mouse ESCs and depletion of CAF-1 in ESCs results in heterochromatin

reorganization and deformation and subsequent lethality (Houlard et al., 2006). In differentiated MEFs, however, CAF-1 depletion had little effect. Because we performed group analysis, we do not rule out important contributions of individual genes inside groups that did not display significant differences between ESCs and NPCs, i.e., chromatin-modifying enzymes. For example, the polycomb group gene Suz12 (an H3K27 HMT) was downregulated following differentiation and was shown to play a role in ESC maintenance (Pasini et al., 2007). In another more recent example, the H3K9me2 and H3K9me3 demethylase genes, Jmjd1a and Jmjd2c, were shown to be positively regulated in ESCs by Oct4, and their depletion results in ESC differentiation (Loh et al., 2007). The changes in individual histone modifier genes may well be responsible for the changes we observed in histone modifications during differentiation. Taken together, our observations strongly point toward an active role of chromatin-remodeling factors in the maintenance of stem cell identity and the initial stages of stem cell differentiation, and are consistent with their disproportionate upregulation in ESCs.

We propose that the higher abundance of chromatin-remodeling factors in ESCs maintains the ESC genome in a preferentially open state allowing freer access of the general transcription machinery and facilitating the stochastic formation of preinitiation complexes (PICs) even on silenced genes. In support of this view, RNA polymerase II complexes are found at promoters of most protein coding genes in ESCs (Guenther et al., 2007). The formation of these PICs might be actively counterbalanced, as the 26S subunit of the proteasome has recently been demonstrated to remove forming PICs from promoters of pluripotent ESCs (Szutorisz et al., 2006). Importantly, no such role for the 26S proteasome was found in differentiated cells, suggesting that the higher propensity of PIC formation is a property of undifferentiated ESCs (Szutorisz et al., 2006). The involvement of the 26S proteasome in removal of the PIC from ESC genes implies that the transcriptional hyperactivity of the ESC genome is under regulatory control. It is unknown at present whether global transcription is merely a by-product of the chromatin properties in ESCs or whether it is essential for pluripotency and control of differentiation, particularly as it is unclear whether the permissive transcripts generated in ESCs are full length and whether they lead to production of functional protein. The possibility that global transcription is functionally important for differentiation is attractive in the light of the observation that in fission yeast heterochromatin silencing is mediated by the RNAi pathway (Volpe et al., 2002) and requires RNA Pol II (Kato et al., 2005). Similar types of mechanisms might be operating in mammalian cells, especially during ESC differentiation, when heterochromatin domains are formed (Meshorer and Misteli, 2006). In support, loss of Dicer, one of the key factors in the RNAi pathway, leads to a significant reduction in heterochromatin silencing in ESCs and to severe defects in ESC differentiation in vitro and in vivo (Kanellopoulou et al., 2005). Similarly, production of noncoding RNAs in ESCs may serve as precursor for regulatory small RNAs (Kapranov et al., 2007). Default global transcription in ESCs may thus be a key mechanism in the maintenance of the pluripotent state and in the silencing of specific genome regions during ESC differentiation.

EXPERIMENTAL PROCEDURES

Cells

Mouse R1 male ESCs (from A. Nagy, Toronto, Canada) were grown and differentiated into 7 day ESC-derived NPCs. The R1 ESC differentiation system has previously been extensively characterized (Lee et al., 2000; Meshorer et al., 2006).

Electron Spectroscopic Imaging

Following immunolabeling, cells were prepared by standard fixation, embedding, and thin sectioning methods (Dellaire et al., 2004). Electron micrographs were taken at 200 kV on a transmission electron microscope (Tecnai 20, FEI). Energy filtered images were collected using a postcolumn imaging filter (Gatan) as described elsewhere (Dellaire et al., 2004).

Antibodies, Western Blots, and Immunofluorescence

Oct4 (goat polyclonal, Santa Cruz Biotechnologies, Santa Cruz, CA, sc-8628); Nestin (rabbit polyclonal, R. McKay); TUJ1 (mouse monoclonal, Chemicon, Temecula, CA, MAB1637); H3K4me3 (rabbit monoclonal, Upstate 05-745); H3K9ac (06-942), H3K14ac (06-911), H3K36me2 (07-274), H3K36me3 (07-549), H3S28p (07-145), and H4K20me2 (06-031) (all rabbit polyclonal, Upstate); and 5-meC (mouse monoclonal, Eurogentec, BI-MECY-0100) antibodies were used. Blots were performed on purified nuclei (Meshorer et al., 2006). Detection was with anti-rabbit or anti-mouse antibodies conjugated to HRP for western blots and either Texas red or FITC (Jackson ImmunoResearch, West Grove, PA) for immunofluorescence (IF). IF was performed as described (Misteli et al., 2000).

Transcription Assay

[^{3}H]uridine was added to the culture media at a final concentration of 3.7 Mbq/ml for 4 hr. Cells were harvested, and RNA and DNA were simultaneously purified using the RNA/DNA Mini Kit (QIAGEN). Messenger RNA was purified using the Oligotex Mini mRNA isolation kit (QIAGEN). Optical density was measured using the ND-1000 spectrophotometer (NanoDrop), and radiation was measured using an LS 6000IC scintillation counter (Beckman).

RNA FISH

Cells grown on gelatin-coated (for ESCs) or poly-L-lysine/fibronectin-coated (for NPCs and PMNs) glass coverslips were treated with CSK buffer (100 mM NaCl, 300 mM sucrose, 3 mM $MgCl_2$, and 10 mM PIPES [pH 6.8]) supplemented with 0.5% Triton X-100 and 200 mM vanadyl ribonucleoside complex (VRC) (Ambion), fixed in 4% paraformaldehyde PBS for 15 min, washed 3× in PBS for 5 min each, and treated in an ascending EtOH series (70%, 80%, 90%, 100%, 5 min each). A locked nucleic acid (LNA) Cy3-labeled 36-mer probe (1 μg/μl) (5′-Cy3-CtCgCcAtAtTtCaCgTcCtAaAgTgTgTaTtTcTc-3′; LNA bases are capitalized) was mixed with unlabeled 18S and 28S rDNA probes (1 μg/μl) (Gift from M. Dundr) and denatured for 5 min at 80°C followed by 30 min at 37°C. Probe was applied overnight in a hybridization solution (50% formamide, 2× SSC, 10% dextran sulfate, and 1 mg/ml BSA) at 37°C in a humidified chamber. Cells were washed 3× in 2× SSC with 50% formamide, then 3× in 2× SSC at 39°C, 5 min each, and in 1× SSC for 5 min at room temperature. Cells were DAPI stained and mounted.

RT-PCR

Bio-Rad MyiQ real-time PCR machine in a 96-well format with IQ SYBR green Supermix (Bio-Rad) was used for all experiments. Reverse transcription was with High Capacity cDNA Archive kit (Applied Biosystems, Foster City, CA) and StrataScript RT-PCR System (Stratagene, Cedar Creek, TX) using 250–1000 ng of total RNA (RNeasy kit supplemented with RNase-free DNase set, QIAGEN, Valencia, CA) with a mix of random hexamers and poly(dT) primers. For quantification, standard curves were generated for each primer pair by serial dilution of the starting template. *Cyclophilin B* was used for normalization. Primers for repetitive sequences and transposable elements were as described elsewhere (Martens et al., 2005). Primers for lineage-specific genes are given in Table S1. Primers for chromatin-remodeling factors are given in Table S4.

Microarray Design and Hybridization

We prepared total poly(A)$^+$ RNA from undifferentiated ESCs, differentiating ESCs at 12 and 24 hr, and 7 day NPCs. Three biological replicates were generated for each time point. Samples were prepared and labeled as described (Kapranov et al., 2002). Briefly, total RNA was enriched for poly(A)$^+$ species using the Oligotex protocol (QIAGEN). Double-stranded cDNA was prepared from poly(A)$^+$ RNA, and 2 μg of double-stranded cDNA was labeled and hybridized to the GeneChip Mouse Tiling Array 1.0R array set (Affymetrix) containing the entire mouse nonrepetitive genome on 16 chips. Sequences used in the design were selected from NCBI mouse genome assembly (Build 32, mm4). Repetitive elements were removed by RepeatMasker. All probes on the chip are tiled at an average resolution of 30 bp, as measured from the central position of adjacent 25-mer oligos, leaving a gap of ~5 bp between probes. All graphs were generated in mouse genome assembly 33 (mm5) using probe coordinates that were remapped to mm5. A total of 192 chips were used for the whole experiment, and composite graphs combining the three biological replica were generated for each time point using standard Affymetrix pipeline (Kampa et al., 2004; Kapranov et al., 2002). All graph files have been submitted to GEO. We first examined whether the signal corresponds to annotated regions and found a perfect correlation between the two. With 5 exons and 4 introns, the stem cell marker *Oct4* serves as an example (Figure S5A, top left). For analysis purpose, only the undifferentiated ESCs and differentiated 7 day NPC samples were used.

Microarray Data Analysis

To generate the number of positive probes in each chromosome (Figure 2), we used the intensity data from the entire set of the mismatch probes (MM) to determine the threshold (χ). We assumed a gamma distribution of the MM intensity values and calculated the mean (μ) and variance (σ). The threshold (χ) was then defined as the intensity level under which 90% of the MM signal is contained. We then counted the number of probes above χ. In order to determine whether the level of expression decreases or increases for the same set of probes between ESCs and NPCs (Figure 4), we compared the expression of all probes in ESCs to all probes in NPCs, filtering out probes below the detection threshold, defined as the threshold that generates a false-positive rate of 2.9% from the bacterial controls on all arrays (Kampa et al., 2004). For a probe to be included in this analysis, it must be present above threshold in both time points. Normalization was done essentially as described (Kampa et al., 2004). Positive probes were determined by the difference (PM-MM) and are thus insensitive to the normalization method, as both PM values and MM values are scaled together.

ACCESSION NUMBERS

The data discussed in this publication have been deposited in NCBI's Gene Expression Omnibus (GEO, http://www.ncbi.nlm.nih.gov/geo/) (Barrett et al., 2007; Edgar et al., 2002) and are accessible through GEO series accession number GSE10834.

SUPPLEMENTAL DATA

Supplemental Data include ten figures, four tables, and Supplemental Experimental Procedures and can be found with this article online at http://www.cellstemcell.com/cgi/content/full/2/5/437/DC1/.

ACKNOWLEDGMENTS

We thank Drs. Liran Carmel (NIH) and Robert Clifford (NIH) for help with statistical analysis, Dr. Mirek Dundr (Boston) for providing rDNA plasmids, and Dr. Bradley Bernstein for the ChIP-seq data shown in Figure S4. This research was supported in part by the Intramural Research Program of the NIH, National Cancer Institute, Center for Cancer Research; the Israel Science Foundation (215/07) (to E.M.); the European Union (IRG-206872) (to E.M.); Alon Fellowship (to E.M.); and an operating grant (to D.P.B.-J.) from the Canadian Institutes of Health Research. D.P.B.-J. holds a Canada Research Chair in Molecular and Cellular Imaging. Design and hybridization of all tiling arrays utilized in this study were supported by Affymetrix, Inc. R.D., J.C., and T.R.G. are employees of Affymetrix, Inc.

Received: June 18, 2007
Revised: November 9, 2007
Accepted: March 28, 2008
Published: May 7, 2008

REFERENCES

Aoto, T., Saitoh, N., Ichimura, T., Niwa, H., and Nakao, M. (2006). Nuclear and chromatin reorganization in the MHC-Oct3/4 locus at developmental phases of embryonic stem cell differentiation. Dev. Biol. *298*, 354–367.

Araki, R., Fukumura, R., Sasaki, N., Kasama, Y., Suzuki, N., Takahashi, H., Tabata, Y., Saito, T., and Abe, M. (2006). More than 40,000 transcripts, including novel and noncoding transcripts, in mouse embryonic stem cells. Stem Cells *24*, 2522–2528.

Arney, K.L., and Fisher, A.G. (2004). Epigenetic aspects of differentiation. J. Cell Sci. *117*, 4355–4363.

Azuara, V., Perry, P., Sauer, S., Spivakov, M., Jorgensen, H.F., John, R.M., Gouti, M., Casanova, M., Warnes, G., Merkenschlager, M., et al. (2006). Chromatin signatures of pluripotent cell lines. Nat. Cell Biol. *8*, 532–538.

Bannister, A.J., Schneider, R., Myers, F.A., Thorne, A.W., Crane-Robinson, C., and Kouzarides, T. (2005). Spatial distribution of di- and tri-methyl lysine 36 of histone H3 at active genes. J. Biol. Chem. *280*, 17732–17736.

Barrett, T., Troup, D.B., Wilhite, S.E., Ledoux, P., Rudnev, D., Evangelista, C., Kim, I.F., Soboleva, A., Tomashevsky, M., and Edgar, R. (2007). NCBI GEO: mining tens of millions of expression profiles—database and tools update. Nucleic Acids Res. *35*, D760–D765.

Bergsland, M., Werme, M., Malewicz, M., Perlmann, T., and Muhr, J. (2006). The establishment of neuronal properties is controlled by Sox4 and Sox11. Genes Dev. *20*, 3475–3486.

Bernstein, B.E., Mikkelsen, T., Xie, X., Kamal, M., Huebert, D., Cuff, J., Fry, B., Meissner, A., Wernig, M., Plath, K., et al. (2006). A bivalent chromatin structure marks key developmental genes in embryonic stem cells. Cell *125*, 315–326.

Bibikova, M., Chudin, E., Wu, B., Zhou, L., Garcia, E.W., Liu, Y., Shin, S., Plaia, T.W., Auerbach, J.M., Arking, D.E., et al. (2006). Human embryonic stem cells have a unique epigenetic signature. Genome Res. *16*, 1075–1083.

Boyer, L.A., Mathur, D., and Jaenisch, R. (2006a). Molecular control of pluripotency. Curr. Opin. Genet. Dev. *16*, 455–462.

Boyer, L.A., Plath, K., Zeitlinger, J., Brambrink, T., Medeiros, L.A., Lee, T.I., Levine, S.S., Wernig, M., Tajonar, A., Ray, M.K., et al. (2006b). Polycomb complexes repress developmental regulators in murine embryonic stem cells. Nature *441*, 349–353.

Bultman, S., Gebuhr, T., Yee, D., La Mantia, C., Nicholson, J., Gilliam, A., Randazzo, F., Metzger, D., Chambon, P., Crabtree, G., et al. (2000). A Brg1 null mutation in the mouse reveals functional differences among mammalian SWI/SNF complexes. Mol. Cell *6*, 1287–1295.

Bultman, S.J., Gebuhr, T.C., Pan, H., Svoboda, P., Schultz, R.M., and Magnuson, T. (2006). Maternal BRG1 regulates zygotic genome activation in the mouse. Genes Dev. *20*, 1744–1754.

Buszczak, M., and Spradling, A.C. (2006). Searching chromatin for stem cell identity. Cell *125*, 233–236.

Cao, S., Bendall, H., Hicks, G.G., Nashabi, A., Sakano, H., Shinkai, Y., Gariglio, M., Oltz, E.M., and Ruley, H.E. (2003). The high-mobility-group box protein SSRP1/T160 is essential for cell viability in day 3.5 mouse embryos. Mol. Cell. Biol. *23*, 5301–5307.

Dellaire, G., Nisman, R., and Bazett-Jones, D.P. (2004). Correlative light and electron spectroscopic imaging of chromatin in situ. Methods Enzymol. *375*, 456–478.

Eckfeldt, C.E., Mendenhall, E.M., and Verfaillie, C.M. (2005). The molecular repertoire of the 'almighty' stem cell. Nat. Rev. Mol. Cell Biol. *6*, 726–737.

Edgar, R., Domrachev, M., and Lash, A.E. (2002). Gene Expression Omnibus: NCBI gene expression and hybridization array data repository. Nucleic Acids Res. *30*, 207–210.

Gan, Q., Yoshida, T., McDonald, O.G., and Owens, G.K. (2007). Concise review: epigenetic mechanisms contribute to pluripotency and cell lineage determination of embryonic stem cells. Stem Cells *25*, 2–9.

Golan-Mashiach, M., Dazard, J.E., Gerecht-Nir, S., Amariglio, N., Fisher, T., Jacob-Hirsch, J., Bielorai, B., Osenberg, S., Barad, O., Getz, G., et al. (2005). Design principle of gene expression used by human stem cells: implication for pluripotency. FASEB J. *19*, 147–149.

Guenther, M.G., Levine, S.S., Boyer, L.A., Jaenisch, R., and Young, R.A. (2007). A chromatin landmark and transcription initiation at most promoters in human cells. Cell *130*, 77–88.

Hochedlinger, K., Yamada, Y., Beard, C., and Jaenisch, R. (2005). Ectopic expression of Oct-4 blocks progenitor-cell differentiation and causes dysplasia in epithelial tissues. Cell *121*, 465–477.

Hough, S.R., Clements, I., Welch, P.J., and Wiederholt, K.A. (2006). Differentiation of mouse embryonic stem cells after RNA interference-mediated silencing of OCT4 and Nanog. Stem Cells *24*, 1467–1475.

Houlard, M., Berlivet, S., Probst, A.V., Quivy, J.P., Hery, P., Almouzni, G., and Gerard, M. (2006). CAF-1 is essential for heterochromatin organization in pluripotent embryonic cells. PLoS Genet. *2*, e181. 10.1371/journal.pgen.0020181.

Hu, M., Krause, D., Greaves, M., Sharkis, S., Dexter, M., Heyworth, C., and Enver, T. (1997). Multilineage gene expression precedes commitment in the hemopoietic system. Genes Dev. *11*, 774–785.

Jorgensen, H.F., Giadrossi, S., Casanova, M., Endoh, M., Koseki, H., Brockdorff, N., and Fisher, A.G. (2006). Stem cells primed for action: polycomb repressive complexes restrain the expression of lineage-specific regulators in embryonic stem cells. Cell Cycle *5*, 1411–1414.

Kaji, K., Caballero, I.M., Macleod, R., Nichols, J., Wilson, V.A., and Hendrich, B. (2006). The NuRD component Mbd3 is required for pluripotency of embryonic stem cells. Nat. Cell Biol. *8*, 285–292.

Kampa, D., Cheng, J., Kapranov, P., Yamanaka, M., Brubaker, S., Cawley, S., Drenkow, J., Piccolboni, A., Bekiranov, S., Helt, G., et al. (2004). Novel RNAs identified from an in-depth analysis of the transcriptome of human chromosomes 21 and 22. Genome Res. *14*, 331–342.

Kanellopoulou, C., Muljo, S.A., Kung, A.L., Ganesan, S., Drapkin, R., Jenuwein, T., Livingston, D.M., and Rajewsky, K. (2005). Dicer-deficient mouse embryonic stem cells are defective in differentiation and centromeric silencing. Genes Dev. *19*, 489–501.

Kapranov, P., Cawley, S.E., Drenkow, J., Bekiranov, S., Strausberg, R.L., Fodor, S.P., and Gingeras, T.R. (2002). Large-scale transcriptional activity in chromosomes 21 and 22. Science *296*, 916–919.

Kapranov, P., Cheng, J., Dike, S., Nix, D.A., Duttagupta, R., Willingham, A.T., Stadler, P.F., Hertel, J., Hackermueller, J., Hofacker, I.L., et al. (2007). RNA maps reveal new RNA classes and a possible function for pervasive transcription. Science *316*, 1484–1488.

Kato, H., Goto, D.B., Martienssen, R.A., Urano, T., Furukawa, K., and Murakami, Y. (2005). RNA polymerase II is required for RNAi-dependent heterochromatin assembly. Science *309*, 467–469.

Kimura, H., Sugaya, K., and Cook, P.R. (2002). The transcription cycle of RNA polymerase II in living cells. J. Cell Biol. *159*, 777–782.

Klochendler-Yeivin, A., Fiette, L., Barra, J., Muchardt, C., Babinet, C., and Yaniv, M. (2000). The murine SNF5/INI1 chromatin remodeling factor is essential for embryonic development and tumor suppression. EMBO Rep. *1*, 500–506.

Kobayakawa, S., Miike, K., Nakao, M., and Abe, K. (2007). Dynamic changes in the epigenomic state and nuclear organization of differentiating mouse embryonic stem cells. Genes Cells *12*, 447–460.

Lee, S.H., Lumelsky, N., Studer, L., Auerbach, J.M., and McKay, R.D. (2000). Efficient generation of midbrain and hindbrain neurons from mouse embryonic stem cells. Nat. Biotechnol. *18*, 675–679.

Lee, T.I., Jenner, R.G., Boyer, L.A., Guenther, M.G., Levine, S.S., Kumar, R.M., Chevalier, B., Johnstone, S.E., Cole, M.F., Isono, K., et al. (2006). Control of developmental regulators by polycomb in human embryonic stem cells. Cell *125*, 301–313.

Loh, Y.H., Zhang, W., Chen, X., George, J., and Ng, H.H. (2007). Jmjd1a and Jmjd2c histone H3 Lys 9 demethylases regulate self-renewal in embryonic stem cells. Genes Dev. *21*, 2545–2557.

Martens, J.H., O'Sullivan, R.J., Braunschweig, U., Opravil, S., Radolf, M., Steinlein, P., and Jenuwein, T. (2005). The profile of repeat-associated histone lysine methylation states in the mouse epigenome. EMBO J. *24*, 800–812.

Meshorer, E. (2007). Chromatin in embryonic stem cell neuronal differentiation. Histol. Histopathol. *22*, 311–319.

Meshorer, E., and Misteli, T. (2006). Chromatin in pluripotent embryonic stem cells and differentiation. Nat. Rev. Mol. Cell Biol. *7*, 540–546.

Meshorer, E., Yellajoshula, D., George, E., Scambler, P.J., Brown, D.T., and Misteli, T. (2006). Hyperdynamic plasticity of chromatin proteins in pluripotent embryonic stem cells. Dev. Cell *10*, 105–116.

Mikkelsen, T.S., Ku, M., Jaffe, D.B., Issac, B., Lieberman, E., Giannoukos, G., Alvarez, P., Brockman, W., Kim, T.K., Koche, R.P., et al. (2007). Genome-wide maps of chromatin state in pluripotent and lineage-committed cells. Nature *448*, 553–560.

Misteli, T., Gunjan, A., Hock, R., Bustin, M., and Brown, D.T. (2000). Dynamic binding of histone H1 to chromatin in living cells. Nature *408*, 877–881.

Nichols, J., Zevnik, B., Anastassiadis, K., Niwa, H., Klewe-Nebenius, D., Chambers, I., Scholer, H., and Smith, A. (1998). Formation of pluripotent stem cells in the mammalian embryo depends on the POU transcription factor Oct4. Cell *95*, 379–391.

Niwa, H. (2007). Open conformation chromatin and pluripotency. Genes Dev. *21*, 2671–2676.

Pan, G.J., Chang, Z.Y., Scholer, H.R., and Pei, D. (2002). Stem cell pluripotency and transcription factor Oct4. Cell Res. *12*, 321–329.

Park, S.H., Kook, M.C., Kim, E.Y., Park, S., and Lim, J.H. (2004). Ultrastructure of human embryonic stem cells and spontaneous and retinoic acid-induced differentiating cells. Ultrastruct. Pathol. *28*, 229–238.

Pasini, D., Bracken, A.P., Hansen, J.B., Capillo, M., and Helin, K. (2007). The polycomb group protein Suz12 is required for embryonic stem cell differentiation. Mol. Cell. Biol. *27*, 3769–3779.

Scholer, H.R., Ruppert, S., Suzuki, N., Chowdhury, K., and Gruss, P. (1990). New type of POU domain in germ line-specific protein Oct-4. Nature *344*, 435–439.

Spivakov, M., and Fisher, A.G. (2007). Epigenetic signatures of stem-cell identity. Nat. Rev. Genet. *8*, 263–271.

Stopka, T., and Skoultchi, A.I. (2003). The ISWI ATPase Snf2h is required for early mouse development. Proc. Natl. Acad. Sci. USA *100*, 14097–14102.

Szutorisz, H., and Dillon, N. (2005). The epigenetic basis for embryonic stem cell pluripotency. Bioessays *27*, 1286–1293.

Szutorisz, H., Georgiou, A., Tora, L., and Dillon, N. (2006). The proteasome restricts permissive transcription at tissue-specific gene loci in embryonic stem cells. Cell *127*, 1375–1388.

Takahashi, K., and Yamanaka, S. (2006). Induction of pluripotent stem cells from mouse embryonic and adult fibroblast cultures by defined factors. Cell *126*, 663–676.

Terskikh, A.V., Miyamoto, T., Chang, C., Diatchenko, L., and Weissman, I.L. (2003). Gene expression analysis of purified hematopoietic stem cells and committed progenitors. Blood *102*, 94–101.

Volpe, T.A., Kidner, C., Hall, I.M., Teng, G., Grewal, S.I., and Martienssen, R.A. (2002). Regulation of heterochromatic silencing and histone H3 lysine-9 methylation by RNAi. Science *297*, 1833–1837.

Xi, R., and Xie, T. (2005). Stem cell self-renewal controlled by chromatin remodeling factors. Science *310*, 1487–1489.

Zipori, D. (2004). The nature of stem cells: state rather than entity. Nat. Rev. Genet. *5*, 873–878.